www.rericjournal.ait.ac.th

Solar Integrated Power Quality Compensator for Cluster of Critical and Sensitive Loads

Ginnes K. John*,[1], M.R. Sindhu*, and T.N.P. Nambiar*

Abstract – *In microgrids, especially after the large scale implementation of power electronics controllers, issues such as distortions, low power factor, imbalances are introduced and these led to higher losses, malfunctioning of controllers, a decline in power quality etc. This paper deals with the performance analysis of a solar integrated power quality shunt compensator for a cluster of critical and sensitive power loads. Power converters are suitably designed to trap the maximum amount of available renewable energy and to feed to the load or to the storage system, which will be then utilized during times of higher load demands. Grid power price increases usually at times of higher load demands. The proposed system is beneficial at this stage as it has the facility to export the power from battery storage to the grid during peak demands. The effectiveness of the controller is tested in an industrial system which consists of AC and DC loads. MATLAB/Simulink simulation studies show the reduction of real, reactive and distortion power burden of the grid in addition to the improvement of power factor and harmonic compensation at the load terminals based on their custom quality of power.*

Keywords – *custom power, distortion power, reactive power, shunt compensator, total harmonic distortion (THD).*

1. INTRODUCTION

Microgrid is defined by the US Department of Energy as "A group of interconnected loads and distributed energy resources within clearly defined electrical boundaries that acts as a single controllable entity with respect to the grid. A microgrid can connect and disconnect from the grid to enable it to operate in both grid-connected or island mode" [1]. The microgrid is also defined by the Consortium for Electric Reliability Technology Solutions (CERTS) as "The MicroGrid concepts assumes an aggregation of loads and micro sources operating as a single system providing both power and heat". The majority of the micro sources must be power electronic based to provide the required flexibility to ensure operation as a single aggregated system. This control flexibility allows the CERTs MicroGrid to present itself to bulk power system as a single control unit that meets the local needs for reliability and security" [2]. In addition to the renewable sources, microgrids have energy storage systems, load control and power quality improvement equipment to ensure reliable power supply, reduce losses, flexibility and good quality to the consumers. Renewable generation includes solar PV systems, wind turbines, fuel cells and bio fueled micro turbines. Batteries and ultra-capacitors are the preferred energy storage systems.

The IEEE P1547 is the frequently used standard for the interconnection of distributed sources to the inter-connected power system [3]. These features are ensured in a microgrid by incorporating peer to peer architecture and plug-and-play concept for each component within the microgrid [2]. The distribution resources help in improving efficiency of the system, as they are local power supplies and, reduces carbon emission, ensures a reduction in losses and utilization of optimal power resources. On the other side, they cause challenging issues such as meshed power flow, bidirectional power flow, increase in fault level, lack of co-ordination of protecting systems, power frequency variations, voltage sag/swell/flicker, harmonics, imbalance, low power factor *etc.*

The testbeds based on the CERTS concept are deployed in real world research projects [4]-[5]. European Union funded MICROGRIDS project report gives the research findings on safe islanding and reconnection practices, challenges in energy managements, control strategies, standard protocols in grid integration and communication systems [6]. Battery storage, fuel cells, photovoltaic cells and micro turbines can be used as DC/AC resources. All DC microgrids are suggested to install DC loads to avoid power conversion losses during AC/DC power conversion [7]. But due to the lack of DC appliances and large grid connected AC/DC converters, hybrid AC/DC microgrids are predominantly employed in applications such as data centers, maritime applications *etc.* Microgrid controller includes control, interfacing and protection of each of the micro resources and control of power flow, load sharing between resources, voltage regulations and stability of the system [8].

Here a microgrid with power sharing among solar power source and utility grid is considered. Loads are classified based on their custom power quality requirement. Critical and sensitive loads need very good quality of supply voltage and in-phase supply current. Hence suitable power quality compensators are to be installed at each of these terminals, which is not a viable option. A unique power quality compensator will be

*Department of Electrical and Electronics Engineering, Amrita School of Engineering, Coimbatore, Amrita Vishwa Vidyapeetham, India.

[1]Corresponding Author;
E-mail: ginneskjohn@gmail.com.

enough to maintain power quality in AC/DC system, if separate feeders can be provided to different categories of custom power loads. This paper presents implementation of solar power quality compensator with an energy storage system to meet customized power quality demand of loads.

2. SYSTEM CONFIGURATION

This section presents an architecture of the microgrid test system as shown in Figure 1. It consists of two feeders with each load comprising different characteristics. The power source in the microgrid is a three phase utility grid (400 V, 50 Hz) and has a solar power source. Induction motors are mainly used in industries due to their ruggedness, easiness in speed control and less maintenance. The induction machines cause reduction in power factor, which may reduce even to 0.5 at no load conditions [9]. These industrial loads are connected as clusters as shown in Figure 1. Here, based on the requirement of quality of power delivered at load terminals, loads are connected to respective feeders- feeder A supplies normal quality loads, which can afford issues such as interruption, harmonics, sag /swell, low power factor *etc*. Feeder B provides good quality of power to critical and sensitive loads. Each of the feeders has circuit breakers which controls the duration of their operation. The microgrid is equipped with a centralized controller which helps to maintain specified power quality at the feeder terminal. The current and voltage signals at each of these feeders are fed back to the centralized controller. This centralized controller, with the help of the selected control strategy, maintains power quality at the feeder B terminals. During situations, where solar power generation is not enough to meet the demanded load, utility meets the load. This causes increase in loss from harmonics and low power factor. The solar power generator is integrated into the grid through three phase VSI [10] at the point of common coupling. Hence the system may be subjected to different type of quality issues- harmonics, interruptions, sag / swell *etc*. A dedicated power quality compensator cum solar integrator is utilized in this work to maintain good power quality at feeder B terminals.

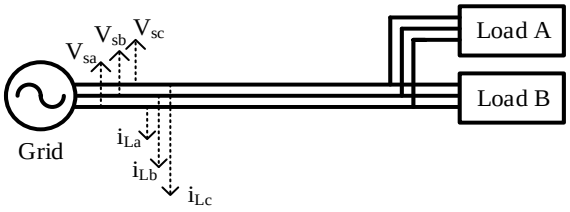

Fig.1. Grid connected test system.

3. OPERATION AND CONTROL OF THE PROPOSED SYSTEM

The block diagram of the controller for the solar integrated compensator is shown in Figure 2. It is operated in two modes, namely mode 1 and mode 2. The solar integrated DC/AC converter is used to meet the real, reactive and distortion power requirement of the loads so that burden on the grid source can be reduced.

3.1 Mode 1

Solar integrated voltage source inverter imports the available amount of solar energy into the system. A portion of the real power demand of the load is supplied by the solar resource. This helps to reduce the power requirement from the utility. At times of high solar irradiance or low load conditions, the solar inverter may supply real power which is more than the requirement of the load. During this period, excess power is fed back to the grid. Three phase reference compensation currents corresponding to solar generated DC current are computed. The hysteresis comparator compares these reference compensation currents and the actual injected currents by the compensator and corresponding gate pulses for the inverter are generated.

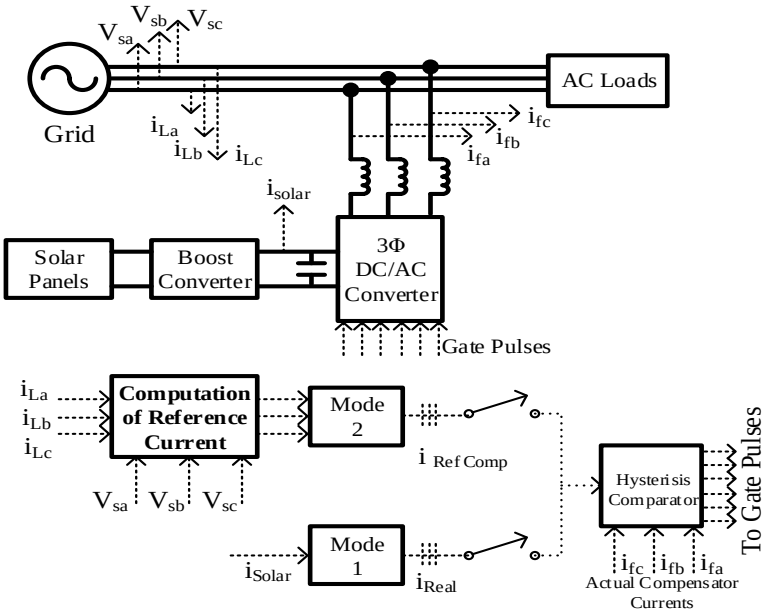

Fig. 2. Controller for the solar integrated compensator.

3.2 Mode 2

In this mode, the inverter works as a solar integrated compensator which supplies real, reactive and distortion power to the load. Linear loads may require only reactive power and a non-linear load needs both reactive and distortion power. In this mode, Icosϕ algorithm [11] is used for the computation of the reference currents to operate inverter as a shunt compensator. These reference currents consist of reactive, harmonic and available portions of real components of load currents. The source voltages and actual load currents are used to calculate the reference current for the compensation. When a critical and sensitive load is connected to the system, it may demand both reactive and distortion power. Solar integrated compensator helps to reduce this burden on the grid. The reference compensation currents and actual compensation currents are compared by the hysteresis comparator to generate gate pulses to the grid integrated solar compensator. This compensation improves both power factor and THD at the feeder terminals which provides good quality of power.

4. SIMULATION ANALYSIS

An industrial test system consists of a variety of loads varying from linear, nonlinear, critical and sensitive loads. For improving efficiency and smoothness in control of loads more and more power electronic controllers were implemented. These controllers introduce power quality issues such as current harmonics, low power factor, increased losses *etc.* The generated harmonics will propagate throughout the system and affects the quality of the voltage at the point of common coupling.

4.1 Case I

In this case study, two different grade quality loads, load A (balanced linear load, unbalanced non-linear load), and load B (unbalanced linear load, critical and sensitive load) are considered. The characteristics of load A and load B are mentioned in Table 1. The behavior of these loads is studied with the help of MATLAB simulation carried out in the system shown in Figure 1 with three phase 400V, 50Hz source. The loads of different categories are introduced into the system as mentioned in Table 1. Each of the loads causes harmonics, reduction in power factor and imbalance. These issues will be propagated throughout the system. The decline in the quality of power at feeder terminals A and B are shown as waveforms in Figure 3 and corresponding values are noted in Table 2. Load current is the resultant current of both quality grade loads. As is evident from the Figure 3, grid currents and load currents are the same.

Table 1. Load characteristics and ratings.

Load and quality grade	Behavior of load	Time instant of switching ON(s)	kVA rating of load
Load A (2 kVA); Conventional Grade	Balanced Linear Load	0.0	0.5
	Unbalanced non-linear Load	0.1	0.5 (Balanced Non-Linear)
	(1.5kVA)	0.06	1 (Unbalanced linear load)
Load B (1kVA); Critical and Sensitive Load	Unbalanced Linear Load	0.06	0.75 (Unbalanced Linear Load)
	Balanced Non Linear Load	0.14	0.25 (Balanced Non Linear Load)

Table 2. System voltage, current, power factor and THD measurements.

Time Interval	0 to 0.06 s	0.06 to 0.1 s			0.1 to 0.14 s			0.14 to 0.2 s		
Phase Parameters	A, B and C	A	B	C	A	B	C	A	B	C
Grid/Load Voltage (rms) (V)	400	400			400			400		
Grid/Load Current (rms) (A)	0.45	2.35	1.7	1.4	4.78	3.2	2.53	5.08	3.87	3.23
Grid/Load Power (VA)	500	616	466	416	1066	66	516	1146	746	597
Grid/Load Power Factor	0.79	0.64	0.643	0.643	0.68	0.6	0.68	0.7	0.7	0.7
THD in %	0.03	0.95	0.84	1.69	18.9	21.5	23.06	23.29	25.63	28.58

During time t = 0 to t = 0.06s, a balanced linear load of 0.5kVA is connected. Grid supplies this load with 0.452A (rms) at 0.794 power factor and THD of 0.03% across all the phases.

Then, at t = 0.06 to 0.1 s, a balanced and unbalanced linear load is connected and grid supplies currents of 2.35A, 1.7A and 1.4A at phases A, B and C respectively. The corresponding power factors are

©2020 Published by RERIC in International Energy Journal (IEJ). Selection and/or peer-reviewed under the responsibility of the Organizers of the **"Artificial Intelligence, Smart Grid and Smart City Applications (AISGSC-2019)"** and the Guest Editors: Dr. L. Ashok Kumar and Dr. R. Latha (PSG College of TechnologyCoimbatore-641 004, Tamilnadu, India.

www.rericjournal.ait.ac.th

0.644, 0.643 and 0.643 respectively at A, B and C phases. During the time interval t = 0.1 to 0.14 s, the balanced non-linear load is connected along with other linear loads and corresponding grid currents are 4.78A, 3.27A and 2.53A. The power factor of 0.68 is measured at all the phases and corresponding grid current THDs are 18.9%, 21.5% and 23.06%.

Finally, from 0.14 to 0.2 s, a critical and sensitive load is connected along with all the other loads. The grid currents are 5.08A, 3.87A and 3.23A, power factors are 0.7, 0.7 and 0.7 and THDs are 23.29%, 25.63% and 28.58% respectively for A, B and C phases. These results show that the quality of power supplied is too low as per IEEE – 519 standards. It is also clear that the system introduces imbalance and low power factor.

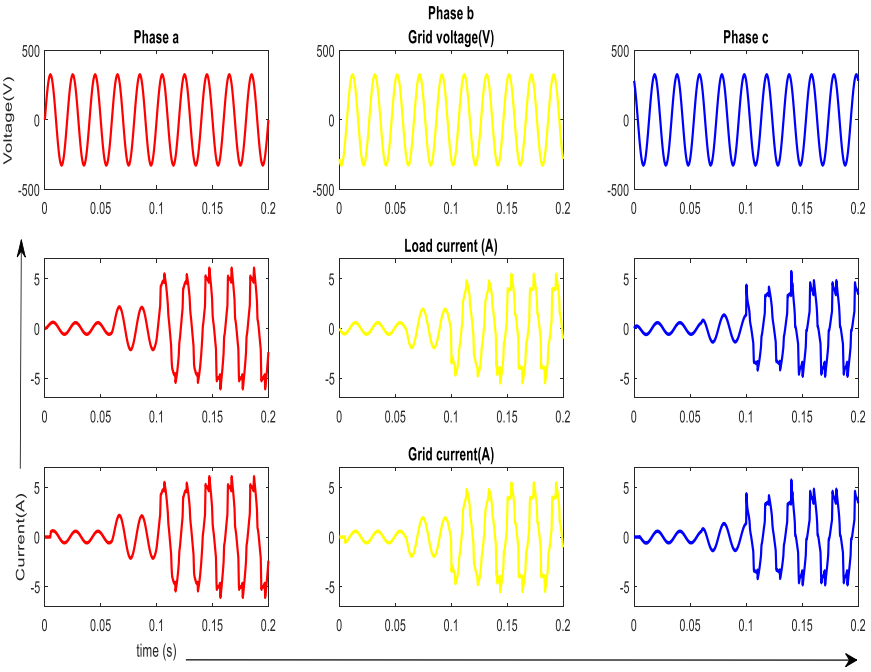

Fig. 3. Three phase grid voltages, load currents and grid currents waveforms – Case I.

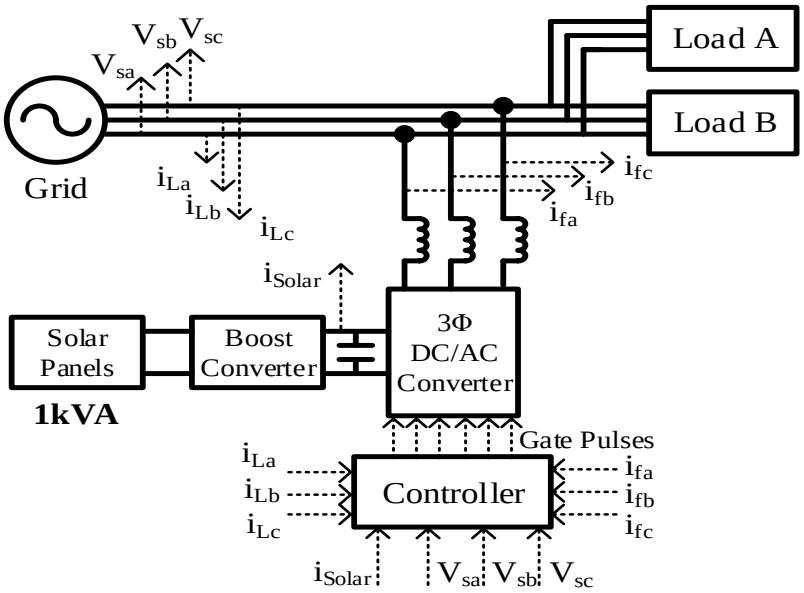

Fig. 4. Solar integrated inverter for AC/DC loads.

4.2 Case II

In this case, as shown in Figure 4, power demand of the load is shared among the grid supply and solar power generation. For simplicity, constant solar irradiance and temperature are assumed. The power tracking circuit is controlled to tap the available solar energy. This solar energy is completely fed to the load terminals. In case

load demand is greater than the available solar power, the deficiency is met with utility power. If the solar power generation exceeds load demand, excess power is imported to the grid. In this paper, in all the cases, time instants of switching of loads are the same as in case I. The DC link voltage is considered as 600V.

During the time interval t = 0 to 0.06 s, out of total demand of balanced linear load 0.5kVA is 100% powered from solar source. The grid receives excess power of 500VA from solar integrated inverter with the current of 0.64A (rms) in each phase. The solar integrated inverter supplies the real power of 0.5kW to the load.

For time interval from t=0.06 to 0.1 s, respective grid currents of phase A, B and C are 1.35A, 0.7A and 0.4A and corresponding THDs are 8.6%, 7.5% and15%.

During the period t=0.1 to 0.14 s, grid currents are measured as 3.78A, 2.27A and 1.53A and its THDs are 14%, 15.9% and 20%, respectively.

During time interval t = 0.14 to 0.2 s, critical and sensitive loads are connected and grid currents of phase A, B and C respectively are 4A, 2.87A and 2.23A and its THDs are 18.69%, 21%, 25.9%, respectively.

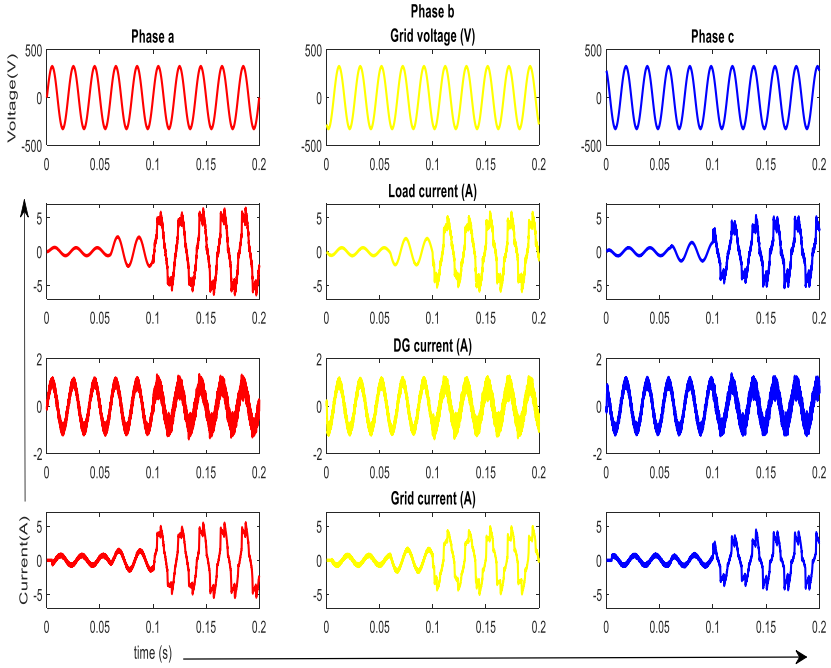

Fig. 5. Three phase grid voltages, load currents, distributed generator currents (DG) and grid currents waveforms – Case II.

Table 3. Case II – Grid/load currents, grid/load/solar power in solar integrated system.

Time Interval	0 to 0.06 s	0.06 to 0.1 s			0.1 to 0.14 s			0.14 to 0.2 s		
Phase Parameters	A, B and C	A	B	C	A	B	C	A	B	C
Grid/Load Voltage (rms)(V)	400		400			400			400	
Grid Current (rms) (V)	-0.64	1.35	0.7	0.4	3.78	2.27	1.53	4	2.87	2.23
Grid Power (VA)	-500	283	133	83	733	333	183	813	413	264
Load voltage (rms) (V)	400		400			400			400	
Load current (rms) (A)	0.4152	2.35	1.7	1.4	4.78	3.27	2.53	5.08	3.57	3.23
Load Power (VA)	500	616	466	416	1066	666	516	1146	746	597
Load Power Factor	0.74	0.644	0.643	0.643	0.68	0.68	0.68	0.7	0.7	0.7
Solar power(W)	500	333	333	333	333	333	333	333	333	333
Grid current THD (%)		8.6	7.5	15.1	14.1	15.9	20.2	18.69	21	25.9

The system quantities measured to ensure real power sharing among the two sources are plotted in Figure 5. Here, as evident from plots in Figure 5, the solar integrated inverter delivers only real power. It does not help in power quality enhancement. Respective system parameters are noted in Table 3. Results show that the solar photovoltaic source provides real power support for the system. Burden on the grid is reduced. Still THDs are not in the limits. Hence, the structure of

©2020 Published by RERIC in International Energy Journal (IEJ). Selection and/or peer-reviewed under the responsibility of the Organizers of the **"Artificial Intelligence, Smart Grid and Smart City Applications (AISGSC-2019)"** and the Guest Editors: Dr. L. Ashok Kumar and Dr. R. Latha (PSG College of TechnologyCoimbatore-641 004, Tamilnadu, India.

www.rericjournal.ait.ac.th

the system is configured with two different feeders of different power quality.

4.3 Case III

In this case, the critical and sensitive load along with an unbalanced linear load of the system is grouped as Load B. Remaining loads are clustered as Load A. Feeders A and B deliver power to Load A and B, respectively. The grid power at available quality is fed to Load A. The Load B requires the utmost quality of power with high reliability. Hence solar power integrator is also utilized also as a power quality enhancer. A constant irradiance and temperature are considered for the simulation. Figure 6 shows the system configuration corresponding to case III. Time instants of switching of loads are the same as in case I and case II. The control algorithm of case III corresponds to the Mode 2 operation of the controller of the solar integrated compensator.

The grid/load/compensator voltage and current waveforms are plotted in Figure 7. Corresponding Feeder B parameters are tabulated in Table 4.

From t = 0 to 0.1 s, the system works as same as case II and from t = 0.1 to 0.2 s, the inverter works as shunt active compensator at the feeder terminal B.

During time interval 0.1 to 0.12 s, Feeder B currents of all phases are 2.09A and its THDs are 8.01%, 8.87% and 8.97% and respective grid current THDs are 12.1%, 13.2% and 18.1%.

From 0.14s onwards critical and sensitive loads are connected to Feeder B and the corresponding Feeder B currents are 2.33 A at phase A, B and C. Imbalance, reactive and distortion power demands of load B are completely met with the solar integrated compensator.

The power factor at Feeder B terminals was improved to 0.99 at all phases. The Grid current THDs are 16.4 %, 19.2% and 21.1 %, respectively. This is due to the distortion introduced by the Load A. The current THDs of Feeder B terminals are evaluated and are 8.18%, 9.17% and 9.23%, respectively. This shows that power quality at Feeder B terminals are improved near to IEEE limits.

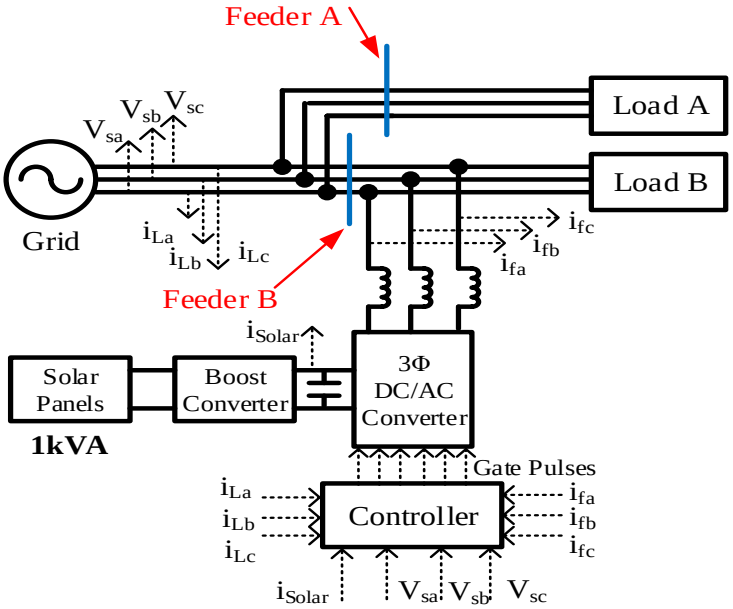

Fig. 6. Solar integrated shunt compensator for power quality enhancement at Feeder B terminals using Icosϕ algorithm.

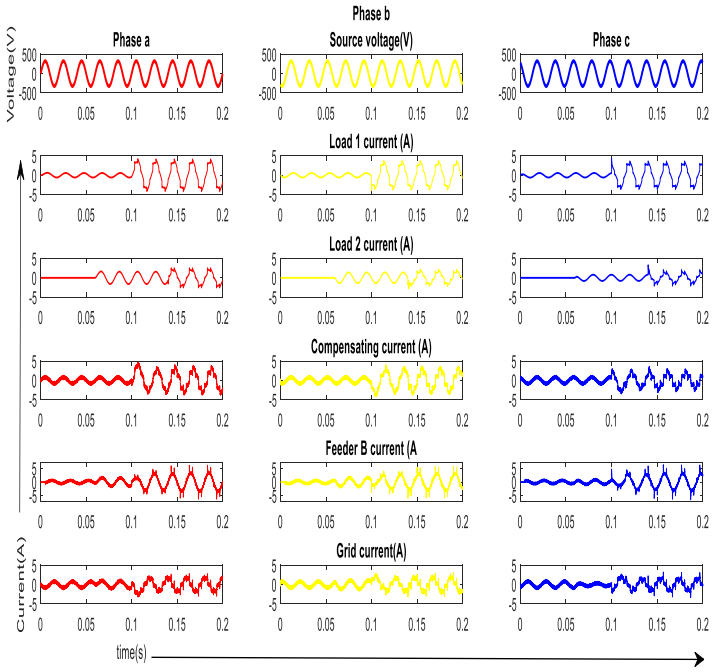

Fig. 7. Three phase grid voltages, load currents, compensating currents, Feeder B currents, and grid currents– Case *III*

The simulation analysis proved that the solar integrated shunt power compensator can be used to inject either real power, distortion and reactive power by using a proper controller algorithm. In this work, the Load B which includes critical and sensitive load is given most priority and its reactive and distortion power is met by solar integrated shunt compensator. The power factors are improved at feeder terminal B and it is also evident from comparison a with case II and case III that after 0.14 s the grid current THDs are also improved because of the distortion and reactive power correction at the feeder terminal B by the shunt compensator.

4.4 Case IV

In this case, the performance of the system under varying solar irradiance is considered. Here, a battery is integrated through a bidirectional buck boost DC/DC converter for energy storage at times of surplus power generation. For a simulation battery bank of 120V, 100 Ah is considered and initially it is near to fully charged. At the time of excess solar power generation, the bidirectional converter will be in buck mode and the battery will be charging. When load demand exceeds the generated solar power, the stored energy in the battery is imported to the loads. At this time bidirectional converter act as boost converter. The schematic diagram of the system is shown in Figure 8. Perturb and observe algorithm based maximum power tracking is employed to control the boost converter.

The solar power source is operated during the time period t = 0 to t = 0.06s and it is assumed that the battery is fully charged. After t = 0.06s, solar irradiance is assumed to be very low and it is not economical to operate the system. Therefore, for the remaining duration, energy stored in the battery is delivered to meet the load demand. The system parameters after the integration of battery storage are tabulated in Table 5.

Table 4. Case III – Solar integrated compensator with Icosϕ algorithm – Feeder B parameters.

Time interval	0.1s to 0.14s			0.14s to 0.2s		
	Phase A	Phase B	Phase C	Phase A	Phase B	Phase C
Feeder B voltage (rms) (V)		400			400	
Feeder B current (rms) (A)	2.09	2.09	2.09	2.33	2.33	2.33
Power Factor at Feeder B	0.99	0.99	0.99	0.99	0.99	0.99
THD at Feeder B (%)	8.01	8.87	8.97	8.18	9.17	9.23
Grid current THD (%)	12.1	13.2	18.1	16.4	19.2	21.1

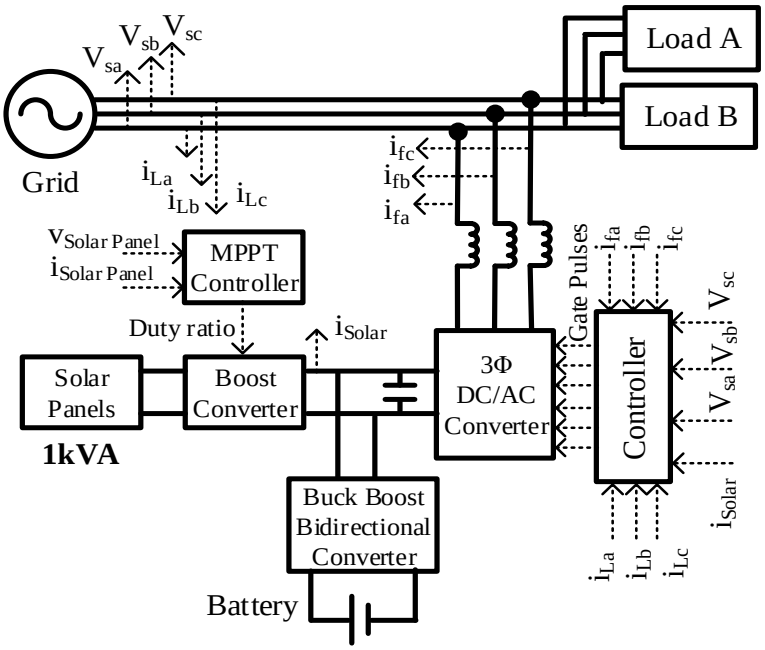

Fig. 8. Solar integrated power quality compensator with energy storage.

The waveforms of the relevant quantities – grid voltages, grid currents, load currents of category A and B, compensator currents, and power supplied by the generator and battery are plotted in Figures 9 and 10, respectively.

Comparing the Tables 3 and 5 values, it can be noted that all values are almost equal except when the solar power is zero after time t = 0.06s. The battery is giving supply to shunt compensator during zero irradiance period.

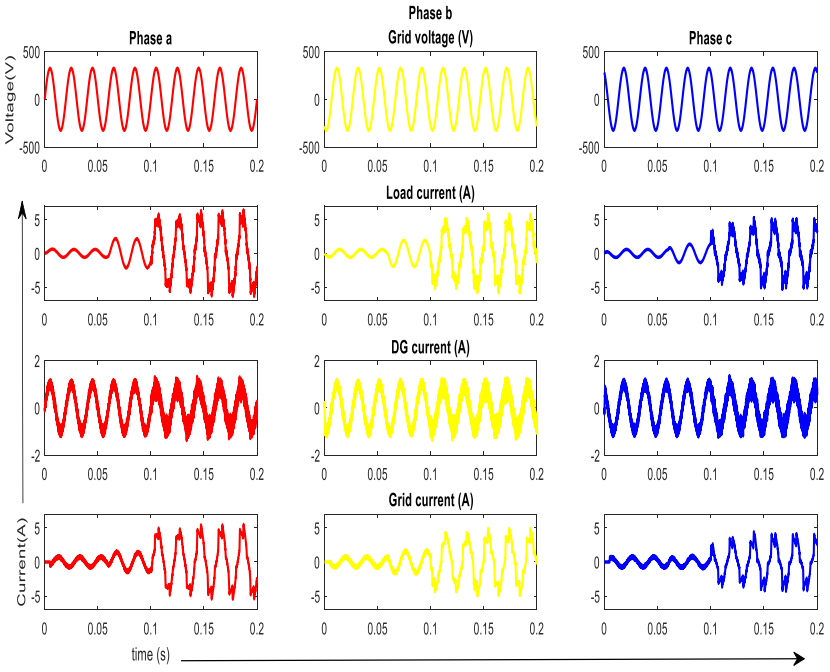

Fig. 9. Three phase grid voltages, load currents, distributed generator currents (DG) and grid currents waveforms – Case IV.

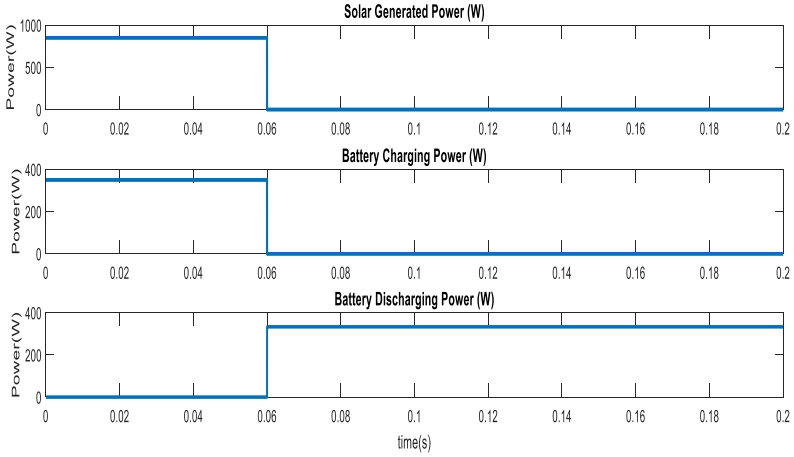

Fig. 10. Solar generated power, battery charging power, battery discharging power waveforms – Case IV.

Table 5. Case IV - Grid/load currents, grid/load/solar/ battery power in solar integrated system.

Time Interval	0 to 0.06 s	0.06 to 0.1 s			0.1 to 0.14 s			0.14 to 0.2s		
Phase Parameters	A, B and C	A	B	C	A	B	C	A	B	C
Grid/Load voltage(rms) (V)	400		400			400			400	
Grid Current (rms) (V)	-0.64	1.35	0.7	0.4	3.78	2.27	1.53	4	2.87	2.23
Grid Power (VA)	-500	283	133	83	733	333	183	813	413	264
Load voltage (rms) (V)	400		400			400			400	
Load current (rms) (A)	0.4152	2.35	1.7	1.4	4.78	3.27	2.53	5.08	3.57	3.23
Load Power (VA)	500	616	466	416	1066	666	516	1146	746	597
Load Power Factor	0.74	0.644	0.643	0.643	0.68	0.68	0.68	0.7	0.7	0.7
Solar Generated power (W)	850	0	0	0	0	0	0	0	0	0
Battery charging Power (W)	350	0	0	0	0	0	0	0	0	0
Battery discharging Power to Load (W)	0	333	333	333	333	333	333	333	333	333
Grid current THD (%)		8.6	7.5	15	14	15.9	20	18.69	21	25.9

4.5 Case V

Here, the battery integrated solar power quality compensator is operated at times of excess solar power generation with respect to load demands. The solar irradiance is assumed to vary in such a way that it increases, reaches the maximum value and decreases as tabulated in Table 6. The results shown in the table verifies that the system maintains power balance at each instant of time. Respective system quantities are shown as waveforms in Figure 11.

The case studies IV and V indicates that the battery controller is effective under varying irradiance conditions.

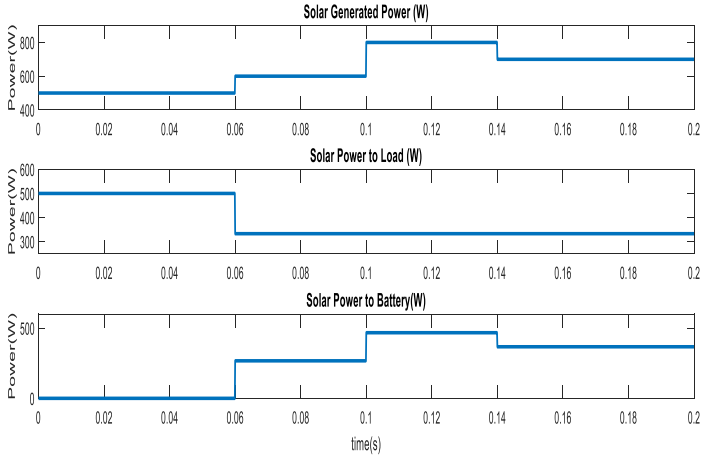

Fig. 11. Solar generated power, solar power to load, solar power to battery waveforms – Case V

Table 6. Case V – Grid/load currents, grid/load/ solar/ battery power in solar integrated system.

Time Interval	0 to 0.06 s	0.06 to 0.1 s			0.1 to 0.14 s			0.14 to 0.2 s		
Phase Parameters	A,B, and C	A	B	C	A	B	C	A	B	C
Grid/Load Voltage (rms) (V)	400		400			400			400	
Grid Current (rms) (A)	-0.64	1.35	0.7	0.4	3.78	2.27	1.53	4	2.87	2.23
Grid Power (VA)	-500	283	133	83	733	333	183	813	413	264
Load voltage (rms) (V)	400		400			400			400	
Load current (rms) (A)	0.4152	2.35	1.7	1.4	4.78	3.27	2.53	5.08	3.57	3.23
Load Power (VA)	500	616	466	416	1066	666	516	1146	746	597
Load Power Factor	0.74	0.644	0.643	0.643	0.68	0.68	0.68	0.7	0.7	0.7
Solar Generated power (W)	500	600	600	600	800	800	800	700	700	700
Solar Power to Load (W)	500	333	333	333	333	333	333	333	333	333
Solar Power to Battery (W)		-267	-267	-267	-467	-467	-467	-367	-367	-367
Grid current THD (%)		8.6	7.5	15	14	15.9	20	18.69	21	25.9

5. COMPARATIVE STUDY WITH OTHER PWM CONTROL ALGORITHM

In this section, the proposed controller for generating real, reactive and harmonics is replaced with conventional instantaneous reactive power theory (IRPT) based control algorithm [12].

The schematic diagram of the system with IRPT controller is shown in Figure 12 and respective waveforms are shown in Figure 13. Relevant system parameters are tabulated in Table 7.

The THD at Feeder B terminals are tabulated from 0.1 to 0.14 s as11.2%, 13.6% and 11.8% respectively for A, B and C phases. From 0.14 to 0.2s the feeder B THD values are 14.2%, 15.4% 15.1% and its corresponding grid current THDs are 17.7%, 20.1% and 22.2%.

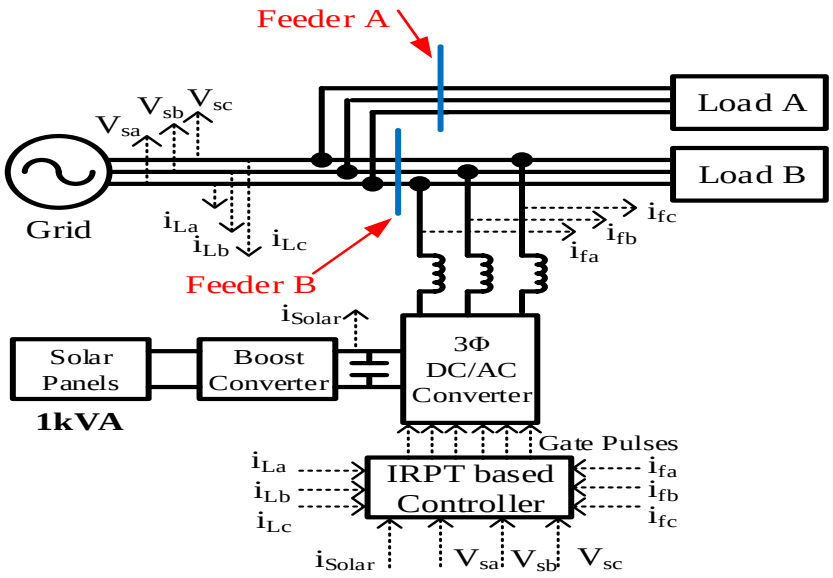

Fig. 12. Solar integrated shunt compensator for power quality enhancement at Feeder B terminals using IRPT algorithm.

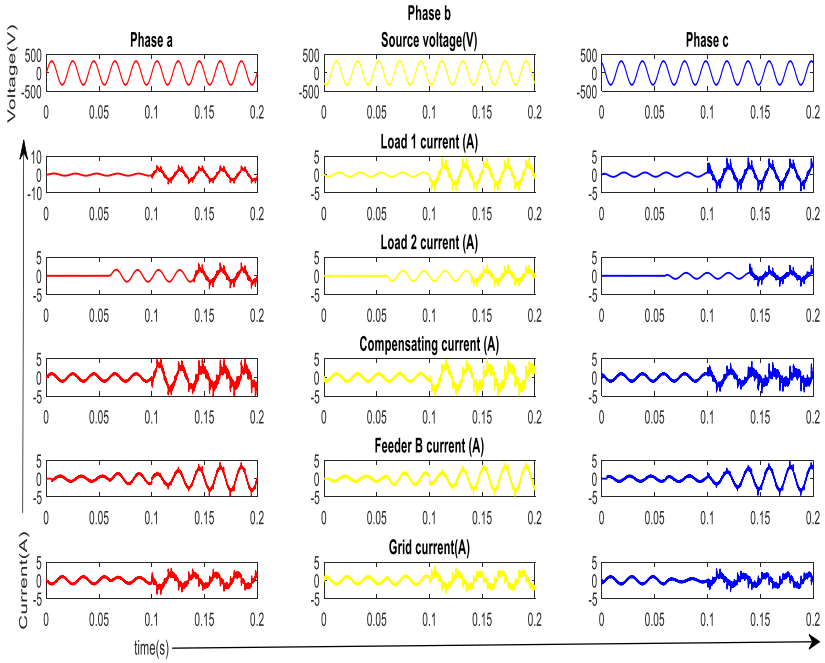

Fig. 13. Three phase grid voltages, load currents, compensating currents, feeder b currents, and grid currents– solar integrated compensator with IRPT algorithm.

Table 7. Solar integrated compensator with IRPT algorithm– Feeder B parameters.

Time interval	0.1s to 0.14s			0.14s to 0.2s		
	Phase A	Phase B	Phase C	Phase A	Phase B	Phase C
Feeder B Voltage (rms) (V)		400			400	
Feeder B Current (rms) (A)	2.22	2.22	2.22	2.64	2.64	2.64
Power Factor at Feeder B	0.99	0.99	0.99	0.99	0.99	0.99
THD at Feeder B	11.2%	13.6%	11.8%	14.2%	15.4%	15.1%
Grid Current THD	12.3%	14.1%	20.4%	17.7%	20.1%	22.2%

Comparing the system performances of both the controllers, it can be seen that performance indices are much better with the proposed compensator system. On the other hand, while considering the complexity of

mathematical operations, the proposed compensator system is much simpler with respect to instantaneous reactive power algorithm. Hence, it can be concluded that the proposed compensator system can provide effective power quality compensation based on custom power demands at the respective load terminals.

6. CONCLUSION

A solar integrated shunt compensator with energy storage for power quality improvement of custom loads in an industry is implemented in this paper. Loads with different characteristics were considered for the study. Simulation analysis shows the enhancement of power quality at the critical and sensitive load terminal. It also adds in utilizing the available solar power to feed loads or to import to the grid. This system also ensures that custom quality of power is available at the respective feeder terminals.

ACKNOWLEDGEMENT

The authors thank Amrita Vishwa Vidyapeetham, Coimbatore, India for their support in carrying out research.

REFERENCES

[1] Ton D.T. and M.A. Smith. 2012. The US department of energy's microgrid initiative. *The Electricity Journal* 25(8): 84–94.

[2] Lasseter R., Akhil A., Marnay C., Stephens J., Dagle J., Guttromson R, et al., 2002. White Paper on Integration of Distributed Energy Resources-The CERTS microgrid concept. *Proceeding of Consortium for Electric Reliability Technology Solutions* 1–27.

[3] Basso T.S. and R.D. DeBlasio. 2003. IEEE P1547-series of standards for interconnection. *IEEE PES Transmission and Distribution Conference and Exposition* 2: 556–561.

[4] Alegria E., Brown T., Minear E., and Lasseter R., 2014. CERTs microgrid demonstration with large scale energy storage and renewable generation. *IEEE Trans. Smart Grid* 5: 937–943.

[5] Panora R., Gehret J., Furse M., and Lasseter R., 2014.Real world performance of a CERT microgrid in Manhattan. *IEEE Transactions on Sustainable energy* 5(4): 1356–1360.

[6] Hatziargyriou N., Jenkins N., Strbac G., Lopes J.A.P., Ruela J., Engler A., Oyarzabal J. Kariniotakis G., and Amorim A., 2006. Microgrids–large scale integration microgeneration to low voltage grids. *CIGRE*.

[7] Hirsch A., Parag Y., and Guerrero J., 2018. Microgrids: A review of technologies, key drives and outstanding issues. *Renewable and Sustainable Energy Reviews* 90: 402–411.

[8] Holf T.E., Wegger H.T., and Farneer B.K., 1996. Distributed generation: An alternative to electric utility investment in system capacity. *Energy Policy* 24(2): 137–147.

[9] Aparna K.J., Sindhu M.R., Jisma M., 2017. Reactive power management of grid connected SCIG using STATCOM. In *Proceedings of International Conference on Circuit, Power and Computing Technologies (ICCPCT)*.pp. 1–5.

[10] Sindhu M.R., Nair M., and Sindhu S., 2016. Photovoltaic based adaptive shunt hybrid filter for power quality enhancement. In *IEEE International Conference on power electronics, drives and energy systems (PEDES)*, Trivandrum, India.

[11] Nair M. and G. Bhuvaneswari. 2005. Design, simulation and analog circuit implementation of a three-phase shunt active filter using the Icosϕ algorithm. In *2005 International Conference on Power Electronics and Drives Energy Systems (PEDES)*.

[12] Akagi J.H., Kanazawa Y. and Nabae A., 1984. Instantaneous reactive power compensators comprising switching devices without energy storage components. *IEEE Transactions Industry Applications* 20(3): 625–630.